J Mater Sci (2008) 43:6505–6512
DOI 10.1007/s10853-008-2931-4

Catalytic activity of CuO-loaded TiO_2/γ-Al_2O_3 for NO Reduction by CO

Jiang Xiaoyuan · Li Huijuan · Zheng Xiaoming

Received: 17 February 2008 / Accepted: 5 August 2008 / Published online: 17 September 2008

Abstract The activities in NO + CO reaction of CuO-loaded TiO_2/γ-Al_2O_3 catalysts prepared by precipitation (P), co-precipitation (C-P), or sol-gel (S-G) were examined using a micro-reactor-gas chromatography (GC) system. The study showed higher catalytic activity of 12%CuO/15%TiO_2/γ-Al_2O_3 (P) than that of 12%CuO/15%TiO_2/γ-Al_2O_3 (S-G) or 12%CuO/15%TiO_2/γ-Al_2O_3 (C-P) in air condition, compared with higher activity of 12%CuO/15%TiO_2/γ-Al_2O_3 (P) or 12%CuO/15%TiO_2/γ-Al_2O_3 (S-G) than that of 12%CuO/15%TiO_2/γ-Al_2O_3 (C-P) in H_2 condition. The specific surface area and crystallite formation had little effect on catalytic activities. H_2-temperature programmed reduction (TPR) revealed four reduction peaks of 12%CuO/15%TiO_2/γ-Al_2O_3 (P), three reduction peaks of 12%CuO/15%TiO_2/γ-Al_2O_3 (S-G), but only one reduction peak of 12%CuO/15%TiO_2/γ-Al_2O_3 (C-P). CuO diffraction peaks were detected only in 12%CuO/15%TiO_2/γ-Al_2O_3 (P), indicating that CuO was highly dispersed on the other two TiO_2/γ-Al_2O_3 catalysts. As a result, 12%CuO/15%TiO_2/γ-Al_2O_3 (P) had the highest activity of reducing NO. During NO + CO reaction, the absorption peaks of intermediate product N_2O were shown at 150 °C by 12%CuO/15%TiO_2/γ-Al_2O_3 (P), at 200 °C by 12%CuO/15%TiO_2/γ-Al_2O_3 (S-G), and at 100 °C by 12%CuO/15%TiO_2/γ-Al_2O_3 (C-P) after H_2 pretreatment at 400 °C for 1 h.

J. Xiaoyuan (✉) · L. Huijuan · Z. Xiaoming
Faculty of Science, Institute of Catalysis, Zhejiang University, Hangzhou 310028, People's Republic of China
e-mail: xyjiang@mail.hz.zj.cn

Introduction

NO_x is one of major air pollutants due to both natural and man-made sources, and controlling NO_x pollution is an urgent task worldwide [1–5]. Since Iwamoto et al. [6] reported selective reduction of NO_x with hydrocarbon in an oxygen-enriched atmosphere by Cu-ZSM-5 and other ionic-exchanged catalysts, many studies on NO reduction have been carried out, e.g. non-selective reduction of NO with CO or selective reduction process of NO with hydrocarbon, transforming NO into harmless N_2. Non-selective reduction of NO with CO is an important method of abating nitrogen oxides, especially in controlling automotive pollutants [7–11].

Recent studies have reported outstanding resistance of TiO_2 to sulfur poisoning and high catalytic activity and selectivity for NO_x abatement. TiO_2 possesses not only low specific surface area but also poor thermal stability, and thus easily transforms from anatase to rutile phase when TiO_2 is heated at 600–800 °C. γ-Al_2O_3 is one of the most common support materials for catalytic purposes, and usually has specific surface areas greater than 200 $m^2\ g^{-1}$, excellent texture, mechanic and thermal properties. TiO_2/Al_2O_3 binary system is regarded as very promising support for $DeNO_x$ catalysts and in many other applications [12–16]. Jason et al. [17] found Au/TiO_2 had higher activity in CO oxidation than Au/Al_2O_3. According to Tamás [18] and Lesage [19], H_2 greatly abated NO, and N_2O was an intermediate product in $NO_x + CO + H_2$ reaction by $Pt/BaO/Al_2O_3$ catalyst. Tatsuo [20] investigated the selective reduction of NO_x with ethanol by Ag/Al_2O_3 and $CuSO_4/TiO_2$, and found that $CuSO_4/TiO_2$ was most effective at removing NH_3, CH_3CN, and HCN simultaneously and reducing NO_x to N_2. It was reported that after addition of TiO_2 to Al_2O_3 the phase-transforming temperature was increased [21], and TiO_2/Al_2O_3 as photo catalyst

greatly degraded 4-nitrobenzene [22]. Macleod et al. [23] found that $Pd/TiO_2/Al_2O_3$ delivered 100% NO_x conversion in $H_2/CO/NO/O_2$ reaction with high oxygen at 100 °C and suggested the synergy between the titania and alumina components caused NO_x conversion. Huang et al. [24] used $Pd–Rh/TiO_2/Al_2O_3$ as a NO_x storage-reduction catalyst in lean-rich cycles, and reported it was highly effective for NO_x reduction and highly resistant to SO_2 and H_2O.

To characterize mixed oxides of titania and alumina, attention should be paid to surface area, pore size distribution, and chemical and physical properties such as morphology, TiO_2 dispersion, and phase distribution. To date, there has been little information about titania-modified aluminas prepared by precipitation, co-precipitation, and sol-gel methods. In the present study, we used a microreactor-GC NO + CO reaction system to examine the catalytic activities of $CuO/TiO_2/\gamma$-Al_2O_3 prepared by the three methods. The analyses were conducted with the BET, H_2-TPR, XRD, Raman, and FT-IR techniques.

Experimental

Preparation of TiO_2/γ-Al_2O_3

TiO_2/γ-Al_2O_3 containing 15% (w/w) of TiO_2 was prepared by precipitation, co-precipitation, or sol-gel methods. In the precipitation method, $TiCl_4$ was dissolved in HCl solution (pH = 5–6), and then added with γ-Al_2O_3 (173 $m^2\ g^{-1}$). Dilute ammonia was dropped into the solution with vigorous stirring until pH = 8.5. The precipitation was kept in the solution at room temperature for 24 h, noted as TiO_2/γ-Al_2O_3 (P). In the co-precipitation method, an aqueous solution of $TiCl_4$ was mixed with $Al(NO_3)_3 \cdot 9H_2O$ reagent. Dilute $NH_3 \cdot H_2O$ was dropped into the mixed solution with magnetic force stirring until pH = 10.5. The Cl^{-1} ions were detected in the two samples after being washed with distilled water. The resulting solid materials were dried at 110 °C in air overnight, and then calcined at 500 °C in air for 2 h, noted as TiO_2/γ-Al_2O_3 (C-P). In the sol-gel method, titanium oxide $[Ti(OC_4H_9)_4]$, ethanol, water, and diethanolamine $[NH(C_2H_5OH)_2]$ were mixed at a molar ratio of 1:26.5:1:1. Al_2O_3 was obtained from the precipitation of $Al(NO_3)_3 \cdot 9H_2O$ with ammonia at pH = 8. After washing with distilled water, the catalysts were dried at 110 °C in air overnight, calcined at 500 °C in air for 2 h, and then added with Al_2O_3 powder to produce TiO_2 sol-gel, noted as TiO_2/γ-Al_2O_3 (S-G).

Preparation of catalysts

Calculated amount of $Cu(NO_3)_2$ solution was soaked with TiO_2/γ-Al_2O_3 prepared as above, and rested for 12 h. After drying in an electric stove, the mixture was calcined at 500 °C in air for 2 h to obtain $CuO/TiO_2/\gamma$-Al_2O_3 catalysts, which had 12%CuO and 15%TiO_2 (w/w).

Measurements of catalytic activity in NO + CO reaction

Catalytic activities were measured using a micro-reactor gas chromatography (GC) reaction system. The system had 5 mm (inside diameter) reaction tube and 30 mL/min of flow velocity of reaction gas, composed of 6%NO, 6%CO, and 88%He (v/v). The amount of catalyst used was 120 mg, and air velocity was set at 5000 h^{-1}. Products of N_2, NO, and CO were detected by a 13× molecular sieve column, and CO_2 and N_2O detected by a Porapak Q column.

Measurements of catalytic properties

Surface areas of catalysts were measured by the BET method based on N_2 adsorption at the liquid-nitrogen temperature using Coulter OMNISORP-100 instrument. Catalysts were degassed at 200 °C in vacuum (10^{-5} Pa) for 2 h.

H_2-temperature programmed reduction (TPR) was done by GC using a thermal conductivity detector. Reduction gases were the mixture of 95%N_2 and 5%H_2 (v/v). TPR was performed with 6 mg of catalysts in temperature range of 80–700 °C at a linear increment of 15 °C/min.

X-ray diffraction (XRD) was measured at 25 °C using a horizontal Rigaku B/Max IIIB powder diffractometer with CuK_α radiation at a power of 40 × 40 mA. The diffraction angle was 2θ (°), and the source wavelength was Cu K_α = 0.15418 nm 0.15° receiving slit, goniometer range at 20–80°, scan speed at 0.2 s/step.

The Raman spectra were taken using a Jobin Yvon Labram HR800 at λ = 514.53 nm, scanning range from 20 to 2000 cm^{-1} and scanning time of 10 s. The lens was 50 × 10.5 with a hole of 250 μm in diameter.

FT-IR spectra were obtained using a Nicolet 560 spectrometer with a MCT detector and a high-pressure, high-temperature DRIFTS cell (Thermo Spectra-Tech) fitted with ZnSe windows. Spectra were acquired from 100 scans at a resolution of 4 cm^{-1}. The sample was treated in hydrogen at 400 °C for 1 h, and then cooled down to room temperature in the same gas to get a background level. After hydrogen was pumped off, the absorbed gas was lead to the IR cell. All spectra were taken at the relevant temperature. The flow rate through the IR cell was 15 mL/min. The absorbed gases contained 10.0%NO + 90%He, 10%CO + 90%He, or 6%NO + 6%CO + 88%He (v/v).

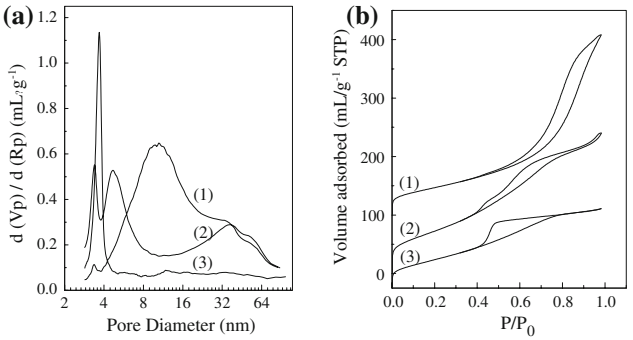

Fig. 1 Adsorption–desorption isotherm and pore size distribution of three types of TiO_2/γ-Al_2O_3. (**a**) Pore size distribution; (**b**) Adsorption–desorption isotherm; (1) TiO_2/γ-Al_2O_3 (P), (2) TiO_2/γ-Al_2O_3 (C-P), (3) TiO_2/γ-Al_2O_3 (S-G)

Results and discussion

Textural and structural properties of TiO_2/γ-Al_2O_3

Pore size distributions of TiO_2/γ-Al_2O_3 prepared by precipitation, co-precipitation, or sol-gel methods belonged to micro-pore and meso-pore (Fig. 1). An earlier study reported that meso-pores were formed during the preparation process and micro-pores became present during the calcining period [25]. It was likely that most of micro-pores existed inside the catalyst, providing the largest portion of specific surface area. The preparation methods had a big effect on specific surface area, which was 265.7 $m^2\ g^{-1}$ in TiO_2/γ-Al_2O_3 (C-P), 171.4 $m^2\ g^{-1}$ in TiO_2/γ-Al_2O_3 (P), and 179.8 $m^2\ g^{-1}$ in TiO_2/γ-Al_2O_3 (S-G) (Table 1). After 12%CuO was loaded onto TiO_2/γ-Al_2O_3, specific surface areas were 131.07 $m^2\ g^{-1}$ by precipitation, 179.10 $m^2\ g^{-1}$ by precipitation, and 142.19 $m^2\ g^{-1}$ by sol-gel. The adsorption–desorption isotherm and pore-size distribution curve of TiO_2/γ-Al_2O_3 were type IV of the BDDT system and typical micro-pore and meso-pore.

TG-DTA measurement

TiO_2/γ-Al_2O_3 prepared by precipitation showed an absorption heat peak at 90 °C, together with an obvious weight-lose step in the TG curve (Fig. 2a). This absorption heat peak could be due to the removal of physical adsorbed H_2O on the sample surface. Moreover, another absorption heat peak occurred at 280 °C, probably due to the decomposition of $Al(OH)_3$ to γ-Al_2O_3 [15, 26]. By comparison, TiO_2/γ-Al_2O_3 prepared by co-precipitation had absorption heat peaks at 440, 600 °C (Fig. 2b). The absorption heat peak at 440 °C might be caused by the transformation of boehmite into γ-Al_2O_3, whereas the peak at 600 °C was likely due to the transformation of anatase into rutile [7]. Preparation by the sol-gel method showed an absorption heat peak at around 500 °C, as a result of the removal of organic substance from the sample surface [15, 25].

Catalytic activities of $CuO/TiO_2/\gamma$-Al_2O_3

The catalytic activities of 12%CuO/15%TiO_2/γ-Al_2O_3 in NO + CO reaction increased with increasing reaction temperatures and also depended upon pretreatment conditions (Fig. 3). With air pretreatment, 100% NO conversion was obtained at 300 °C by 12%CuO/15%TiO_2/γ-Al_2O_3 (P) and at 350 °C by other two catalysts. Pretreatment with H_2 at 400 °C for 1 h markedly increased catalytic activities, and 100% NO conversion occurred at 275 °C for 12%CuO/15%TiO_2/γ-Al_2O_3 (S-G) and 12%CuO/15%TiO_2/γ-Al_2O_3 (P), compared with 300 °C for 12%CuO/15%TiO_2/γ-Al_2O_3 (C-P). The increased activities after H_2 pretreatment were probably due to, (1) adsorbed H_2 by the catalysts directly involved in NO + CO reaction, as previously reported by Isabella [27]; 2) H_2 reduction caused changes in active phase species. After H_2 pretreatment, the copper species mostly existed as Cu^0 and Cu^+, and Cu^+ was the catalytic activity center in NO + CO reaction [28, 29].

H_2-TPR measurement

Compared with one single peak at 350 °C by pure CuO, there were four reduction peaks (namely α, β, γ, and δ) at 177.6, 190.4, 218.9, and 262.2 °C by 12%CuO/15%TiO_2/γ-Al_2O_3 (P); one reduction peak at 223 °C by 12%CuO/15%TiO_2/γ-Al_2O_3 (C-P);and three reduction peaks at 295.5, 392.4, and 430 °C by 12%CuO/15%TiO_2/γ-Al_2O_3 (S-G) (Fig. 4). According to Hu et al [30, 31], when the amount of TiO_2 was less than 0.56 mmol Ti^{4+}/100 m^2 γ-Al_2O_3, the dispersion of CuO on TiO_2/γ-Al_2O_3 was largely affected by surface Ti^{4+}. Since the interaction of CuO with TiO_2 was greater than with γ-Al_2O_3, some of the dispersed Cu^{2+} ions might occupy the vacant sites of TiO_2. In Xu's model [32], anatase surface (001) was filled with highly dispersed CuO. When CuO loadings were in the

Table 1 Specific surface areas and pore volumes of TiO_2/γ-Al_2O_3 prepared by three methods

	TiO_2/γ-Al_2O_3 (P)	TiO_2/γ-Al_2O_3 (C-P)	TiO_2/γ-Al_2O_3 (S-G)
Specific surface area ($m^2\ g^{-1}$)	171.4	265.7	179.8
Pore volume (mL g^{-1})	0.497	0.352	0.199
Average pore size (nm)	12.00	9.42	6.42

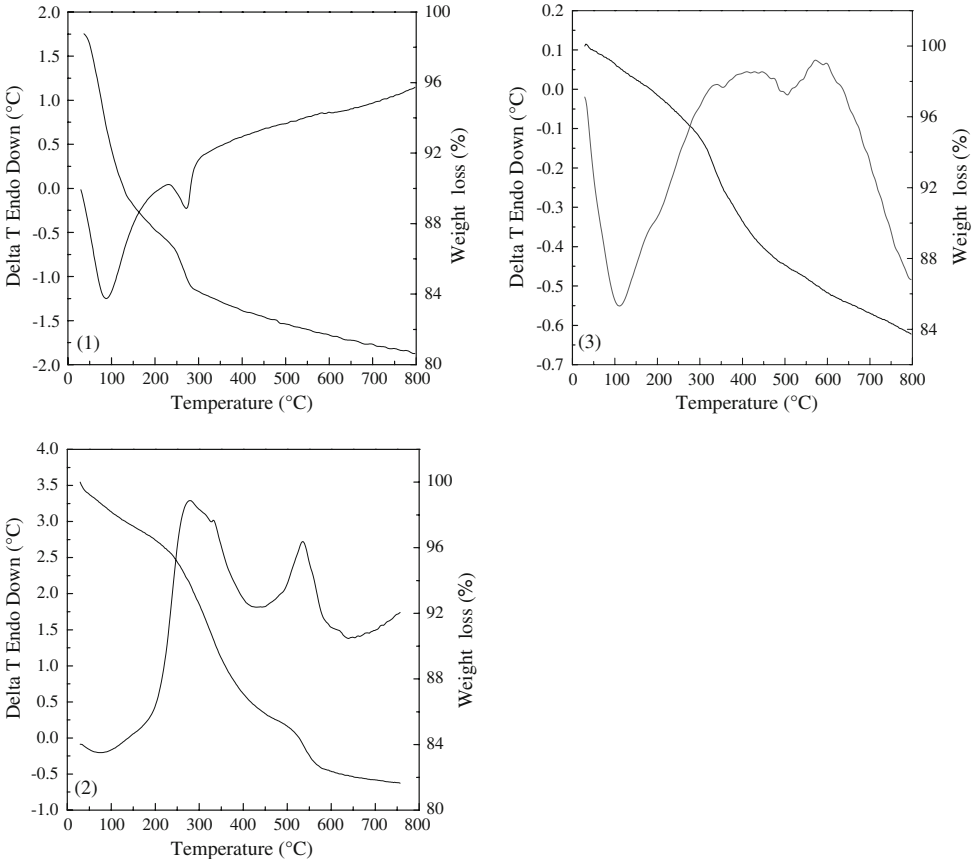

Fig. 2 TG-DTA patterns of three types of TiO_2/γ-Al_2O_3 in air atmosphere; (1) TiO_2/γ-Al_2O_3 (P), (2) TiO_2/γ-Al_2O_3 (C-P), (3) TiO_2/γ-Al_2O_3 (S-G)

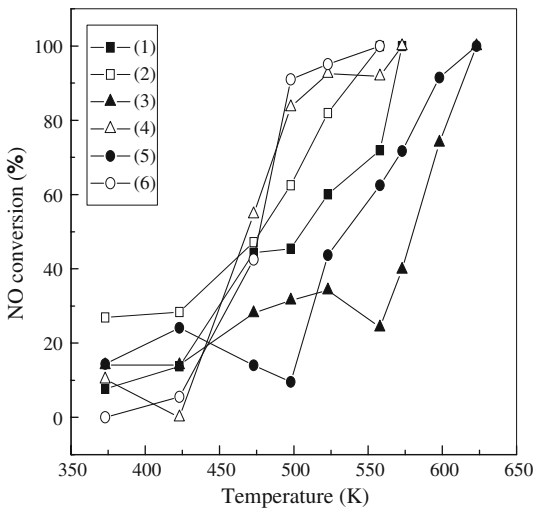

Fig. 3 Catalytic activity of 12%CuO/15%TiO_2/γ-Al_2O_3 in NO + CO reaction; (1) P (pretreated in air), (2) P (pretreated in H_2), (3) C-P (pretreated in air), (4) C-P (pretreated in H_2), (5) S-G (pretreated in air), (6) S-G (pretreated in H_2)

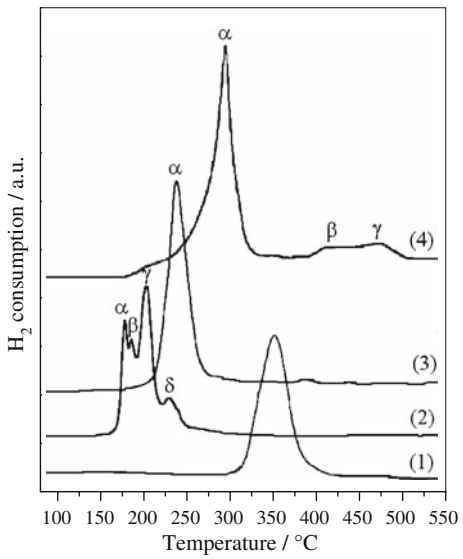

Fig. 4 H_2-TPR profiles of (1) CuO, (2) 12%CuO/15%TiO_2/γ-Al_2O_3 (P), (3) 12%CuO/15%TiO_2/γ-Al_2O_3 (C-P), and (4) 12%CuO/15% TiO_2/γ-Al_2O_3 (S-G)

range of 1.81–17.82Cu^{2+} nm^{2-} (equal to 1.13–11.13 wt%), CuO existed in two phases, i.e. dispersed CuO and crystalline CuO [33].

The α and γ peaks of 12%CuO/15%TiO_2/γ-Al_2O_3 (P) were the reductions of crystalline CuO and highly dispersed CuO on naked TiO_2 of TiO_2/γ-Al_2O_3, respectively. The β and δ peaks were the reductions of crystal CuO and highly dispersed CuO on TiO_2/γ-Al_2O_3, respectively. The only one peak of 12%CuO/15%TiO_2/γ-Al_2O_3

(C-P) was attributed to highly dispersed CuO at the surface of naked γ-Al_2O_3. The α peak of 12%CuO/15%TiO_2/γ-Al_2O_3 (S-G) was the reduction of dispersed CuO on the anatase surface of TiO_2/γ-Al_2O_3, whereas the β and γ peaks were the reduction of TiO_2/γ-Al_2O_3. The α peaks of 12%CuO/15%TiO_2/γ-Al_2O_3 (C-P) and 12%CuO/15%TiO_2/γ-Al_2O_3 (S-G) were large and likely had covered other reduction peaks. XRD results also showed diffraction peaks of both TiO_2 and γ-Al_2O_3 by TiO_2/γ-Al_2O_3 (P), but only γ-Al_2O_3 peak by TiO_2/γ-Al_2O_3 (C-P) and intensive TiO_2 peak and weak γ-Al_2O_3 peak by TiO_2/γ-Al_2O_3 (S-G). The Raman peak of CuO was detected in 12%CuO/15%TiO_2/γ-Al_2O_3 (P) only, indicating crystalline CuO on catalyst surface. CuO was highly dispersed on the surfaces of TiO_2/γ-Al_2O_3 (C-P) and TiO_2/γ-Al_2O_3 (S-G). The Raman peak of TiO_2 by 12%CuO/15%TiO_2/γ-Al_2O_3 (S-G) was much more intensive than that by 12%CuO/15%TiO_2/γ-Al_2O_3 (P), suggesting massive crystalline TiO_2 on CuO/TiO_2/γ-Al_2O_3 (S-G), massive γ-Al_2O_3 on TiO_2/γ-Al_2O_3 (P), and highly dispersed TiO_2.

XRD measurement

TiO_2/γ-Al_2O_3 (P) clearly showed the anatase and γ-Al_2O_3 phase (Fig. 5). Wei et al. [34] found that TiO_2 covered less than 50% of γ-Al_2O_3 surface area in TiO_2/γ-Al_2O_3 (P) and the uncovered γ-Al_2O_3 could be detected by XRD. In this study, TiO_2/γ-Al_2O_3 (C-P) had no obvious diffraction peaks of the anatase, indicating that titania was highly dispersed on the alumina support. Vargas et al. [35] reported that anatase was highly dispersed on TiO_2/γ-Al_2O_3 or formed undetectable crystalline ($d < 4$ nm). In the present study, TiO_2/γ-Al_2O_3 (S-G) showed obvious diffraction peak of anatase but weak diffraction peak of γ-Al_2O_3. This may indicate that amorphous Al_2O_3 was highly dispersed on TiO_2, and γ-Al_2O_3 had not yet formed. Similarly, Pt-Rh/TiO_2/Al_2O_3 was highly effective in NO_x reduction and highly resistant to SO_2 and H_2O [24]. According to Hernadez and Bautista [15], TiO_2 modified the structure of γ-Al_2O_3 at <450 °C, and weak γ-Al_2O_3 crystalline diffraction peaks and obvious anatase phase were detected. It was suggested that TiO_2/γ-Al_2O_3 prepared by sol-gel mostly formed amorphous Al_2O_3 but not γ-Al_2O_3 phase at low temperature.

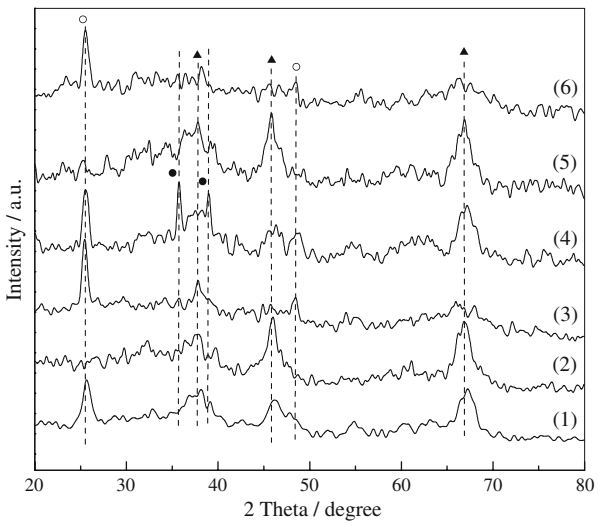

Fig. 5 XRD patterns of different TiO_2/γ-Al_2O_3 catalysts; ○ TiO_2 ▲ γ-Al_2O_3 ● CuO; (1) 15%TiO_2/γ-Al_2O_3 (P), (2) 15%TiO_2/γ-Al_2O_3 (C-P), (3) 15%TiO_2/γ-Al_2O_3 (S-G), (4) 12%CuO/15%TiO_2/γ-Al_2O_3 (P), (5) 12%CuO/15%TiO_2/γ-Al_2O_3 (C-P), (6) 12%CuO/15%TiO_2/γ-Al_2O_3 (S-G)

Obvious CuO diffraction peaks were detected in 12%CuO/15%TiO_2/γ-Al_2O_3 (P), compared with highly dispersed CuO on the catalysts prepared by the co-precipitation or sol-gel method. Moreover, 12%CuO/15%TiO_2/γ-Al_2O_3 (P) had the highest activities in NO + CO reaction. Luo et al. [36] found that the activity of CuO/Al_2O_3 in CO oxidation also increased with increasing CuO loading, probably as a result of highly dispersed CuO and bulk CuO species. Jiang et al. [37] also reported highly dispersed CuO and fine grain CuO species in NO + CO reaction by CuO–ZrO_2/TiO_2. It may be concluded that highly dispersed CuO was the main active center and crystalline CuO enhanced the catalytic activity.

Raman measurement

Since most of laser light entering into samples is absorbed, the Raman spectra can be used to analyze the surface of the samples [36, 37]. Compared with a combined signal given by XRD, the Raman peaks provide both surface and bulk phase information. When samples strongly absorb laser light, the signals of bulk phase will be weakened and the Raman spectra mainly show the surface phase information. In this study, CuO had four peaks at 284, 345, 620, and 1106 cm^{-1} (Fig. 6). No crystalline CuO Raman peaks were detected in CuO-loaded TiO_2/γ-Al_2O_3 prepared by co-precipitation or sol-gel method, indicating that CuO was highly dispersed on TiO_2/γ-Al_2O_3. While 12%CuO/15%TiO_2/γ-Al_2O_3 (S-G) and 12%CuO/15%TiO_2/γ-Al_2O_3 (P) had intensive TiO_2 Raman peaks, 12%CuO/15%TiO_2/γ-Al_2O_3 (C-P) had a very weak peak probably due to its large surface area and highly dispersed CuO and TiO_2.

FT-IR measurement

At low temperatures, 12%CuO/15%TiO_2/γ-Al_2O_3 (P) absorbed CO and NO independently (Fig. 7a). Two strong peaks of NO adsorption occurred at 1840, 1907 cm^{-1} and increased with increasing temperatures, but faded away at >200 °C. The CO absorption peaks occurred at 2115 and

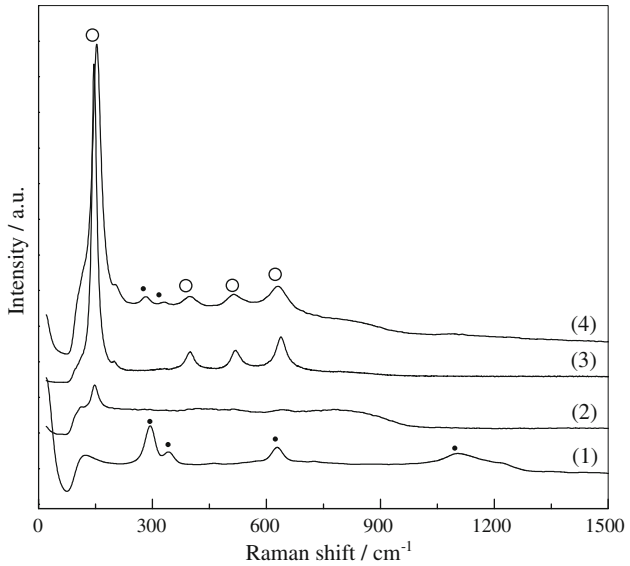

Fig. 6 Raman spectra of CuO and CuO-loaded TiO_2/γ-Al_2O_3 catalysts; ○ TiO_2 ● CuO; (1) CuO, (2) 12%CuO/15%TiO_2/γ-Al_2O_3 (C-P), (3) 12%CuO/15%TiO_2/γ-Al_2O_3 (S-G), (4) 12%CuO/15%TiO_2/γ-Al_2O_3 (P)

2174 cm^{-1} and decreased gradually with increasing temperatures. The adsorption peaks at 2337 and 2362 cm^{-1} were attributed to CO_2 adsorption. This may relate to the release of CO_2 during NO + CO reaction. Higher temperature produced more CO_2, and thus stronger CO_2 adsorption bands [38]. At 200 °C, the adsorption band was shifted from 2174 to 2190 cm^{-1}, plus new adsorption band at 2210 cm^{-1}. At 150 °C the N_2O adsorption band appeared at 2337 cm^{-1}, and increased with increasing temperature until 250 °C, and then weakened quickly and disappeared at about 400 °C. It was likely that in the reactions N_2O was produced at low temperature but turned into final product N_2 at high temperature. This was consistent with the activities of 12%CuO/15%TiO_2/γ-Al_2O_3 (P) measured by microreactor-GC in NO + CO reaction. N_2O formation was due to NO decomposition and combination of N and NO on the catalyst surface. Similarly, combination of O and NO produced NO_2 or NO_x(x = 2–3). Bands at 1394 and 1450 cm^{-1} belonged to nitrate adsorption [39] and the two peaks fade away with rising temperature. Small bands of carbonate and bicarbonate were also observed in the region of 1500–1750 cm^{-1} but disappeared with rising temperature, indicating that CO_2 released in NO + CO reaction might have reacted with Cu^{2+} and other metal oxides. Carbonate and bicarbonate are considered as the intermediate of CO oxidation [40, 41].

Catalysts 12%CuO/15%TiO_2/γ-Al_2O_3 (C-P) and 12% CuO/15%TiO_2/γ-Al_2O_3 (S-G) had similar peaks of absorption (Fig. 7b, c), and their NO and CO adsorption bands were the same as that of 12%CuO/15%TiO_2/γ-Al_2O_3 (P). The bands at 1604 and 1630 cm^{-1} were due to NO_2 adsorption and decreased with increasing temperature. The peak at 1300 cm^{-1} was of nitrate adsorption on the catalyst surface. At low temperature, some of absorbed NO reacted with O_2 to form NO_2 and the remaining NO reacted with the species on the catalyst surface to form carbonate and bicarbonate. At 150 °C, 12%CuO/15%TiO_2/γ-Al_2O_3 (C-P) had a weak adsorption of N_2O at 2235 cm^{-1}. The band became large with increasing temperature and reached maximum at 250 °C, but disappeared at 400 °C. In contrast, 12%CuO/15%TiO_2/γ-Al_2O_3 (S-G) showed an obvious absorption peak of N_2O at 100 °C.

Numerous studies have been conducted to clarify the absorption band at 2210 cm^{-1}. Novak et al. [42] examined NO + CO reaction by Rh-loaded catalyst and assigned the bands at 2175–2180 cm^{-1} as Rh-NCO^- adsorption. London [43] considered the band at 2200 cm^{-1} as the Cu^0-NCO^- species, while other researchers [8, 44–46] assumed the peaks at 2150–2200 cm^{-1} as M-NCO(M denotes the metal ion)species. It may be suggested that NCO structure always appeared in NO + CO reaction by the catalysts loaded with transition metal oxides at high temperature. In this study, the absorption peak occurred at 2210 cm^{-1} only when catalysts were pretreated with H_2, and Cu^0 and Cu^+ species were formed on the catalyst surface. We assigned the band at 2210 cm^{-1} as the absorption of Cu^0-NCO^-. Different FT-IR spectra of absorbed NO + CO gases were shown between the CuO-loaded TiO_2/γ-Al_2O_3 catalysts prepared by different methods with H_2 pretreatment. N_2O absorption peak was detected at 100 °C for 12%CuO/15%TiO_2/γ-Al_2O_3 (S-G), at 150 °C for 12%CuO/15%TiO_2/γ-Al_2O_3 (P), and at 200 °C for 12%CuO/15%TiO_2/γ-Al_2O_3 (C-P). As N_2O is the key intermediate product in NO + CO reaction, its appearance and disappearance directly affect the rate of reaction and NO conversion. Therefore, it is very important to detect the N_2O appearance temperature.

Conclusions

(1) 12%CuO/15%TiO_2/γ-Al_2O_3 (P) had high activity in NO + CO reaction, and achieved 100% NO conversion at 300 °C. When the catalyst was pretreated with H_2, the NO conversion reached 100% at 275 °C.

(2) There were four reduction peaks (α, β, γ, and δ) by 12%CuO/15%TiO_2/γ-Al_2O_3 (P). The α and γ reduction peaks belonged to highly dispersed CuO and crystalline CuO on the exposed TiO_2, respectively. The β and δ peaks were the reductions of highly dispersed CuO and crystalline CuO on TiO_2/γ-Al_2O_3, respectively. 12%CuO/TiO_2/γ-Al_2O_3 (C-P) had only one reduction peak of CuO on the exposed γ-Al_2O_3. Three reduction peaks (α, β, and γ) were shown by 12%CuO/15%TiO_2/γ-Al_2O_3 (S-G). The α peak was

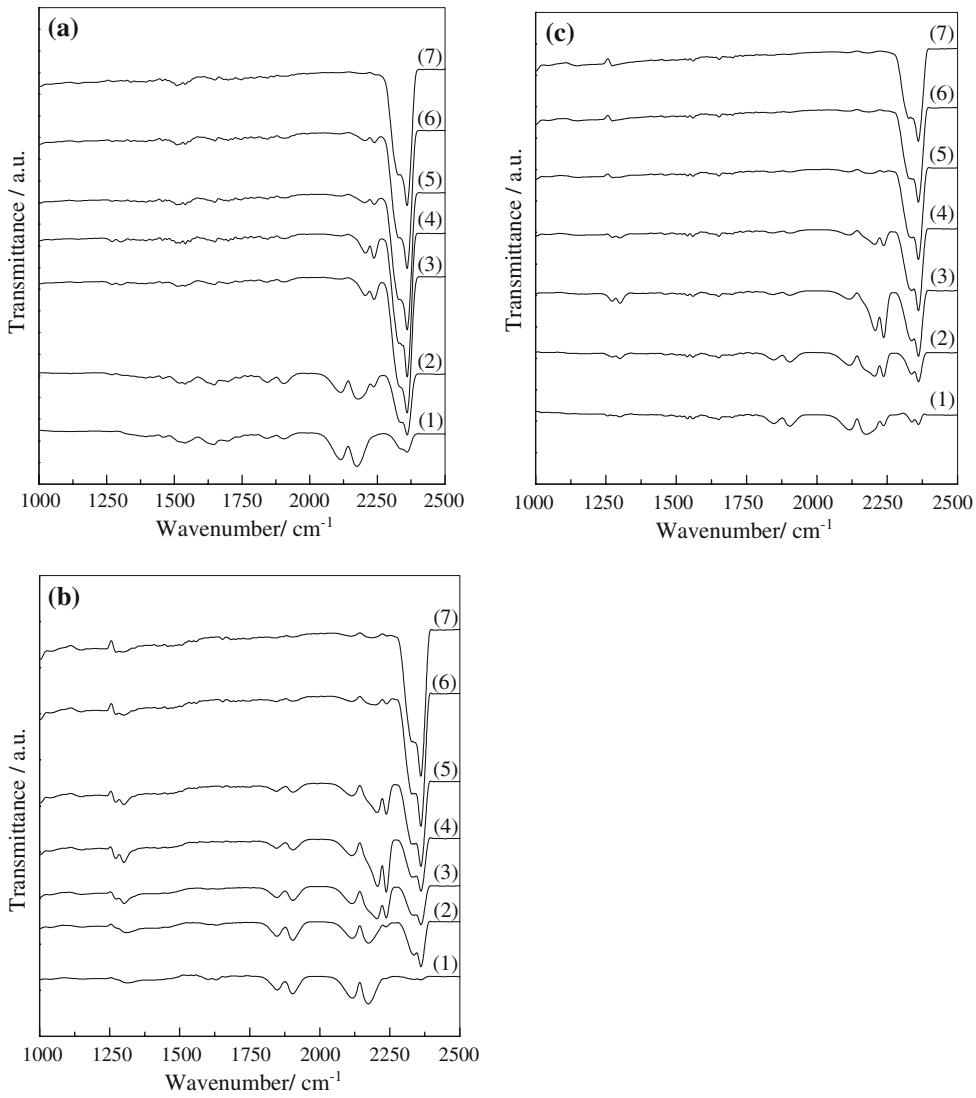

Fig. 7 FT-IR spectra of NO + CO absorbed on three kinds catalysts pretreating by H_2; (**a**) (1) 100 °C, (2) 150 °C, (3) 200 °C, (4) 250 °C, (5) 300 °C, (6) 350 °C, (7) 400 °C; (**b**) (1) 100 °C, (2) 150 °C, (3) 200 °C, (4) 250 °C, (5) 300 °C, (6) 350 °C, (7) 400 °C; (**c**) (1) 100 °C, (2) 150 °C, (3) 200 °C, (4) 250 °C, (5) 300 °C, (6) 350 °C, (7) 400 °C

the reduction of CuO on the exposed TiO_2, and the β and γ peaks were the reductions of TiO_2/γ-Al_2O_3.

(3) CuO diffraction and Raman peaks were detected in 12%CuO/15%TiO_2/γ-Al_2O_3 (P) but not in 12%CuO/TiO_2/γ-Al_2O_3 (C-P) and 12%CuO/15%TiO_2/γ-Al_2O_3 (S-G), indicating that CuO phase was highly dispersed on the latter two catalysts.

(4) In NO + CO reaction, the absorption peaks of intermediate product N_2O were shown at 150 °C by 12%CuO/15%TiO_2/γ-Al_2O_3 (P), at 200 °C by 12% CuO/15%TiO_2/γ-Al_2O_3 (S-G), and at 100 °C by 12% CuO/15%TiO_2/γ-Al_2O_3 (C-P) after H_2 pretreatment at 400 °C for 1 h.

Acknowledgement The authors acknowledge financial support from the Natural Science Foundation of Zhejiang Province, China (Y504131).

References

1. Went GT, Leu LJ, Rosin RR (1992) J Catal 134:492. doi:10.1016/0021-9517(92)90337-H
2. Fritz A, Pitchon V (1997) Appl Catal B Environ 13:1. doi:10.1016/S0926-3373(96)00102-6
3. Pârvulescu VI, Grange P, Delmon B (1998) Catal Today 46:233. doi:10.1016/S0920-5861(98)00399-X
4. Busca G, Lietti L, Ramis G, Bertl F (1998) Appl Catal B Environ 18:1
5. Giakoumelou I, Fountzoula C, Kordulis C, Boghosian S (2006) J Catal 239:1. doi:10.1016/j.jcat.2006.01.019
6. Iwamoto M, Yahiro H, Torikai Y (1990) Chem Lett 19:1967. doi:10.1246/cl.1990.1967
7. Wollner A, Lange F (1993) Appl Catal Gen 94:181. doi:10.1016/0926-860X(93)85007-C
8. Larsson PO, Andersson A, Wallenberg L (1996) J Catal 163:279. doi:10.1006/jcat.1996.0329
9. Amano F, Suzuki S, Yamamoto T, Tanaka T (2006) Appl Catal B Environ 64:282. doi:10.1016/j.apcatb.2005.12.011

10. Jiang XY, Ding GH, Lou LP, Chen YX, Zheng XM (2004) Catal Today 93:811. doi:10.1016/j.cattod.2004.06.074
11. Schneider H, Tschudin S, Schneider M (1994) J Catal 147:8
12. Santes V, Herbert J, Cortez MT (2005) Appl Catal Gen 281:121. doi:10.1016/j.apcata.2004.11.025
13. Kaneko EY, Pulcinelli SH, Silva VTD, Santilli CV (2002) Appl Catal Gen 235:74. doi:10.1016/S0926-860X(02)00236-3
14. Öhman LO, Paul J (2002) Mater Chem Phys 73:246
15. Hernadez T, Bautista MC (2005) J Eur Ceram Soc 25:668
16. Chidamaram PR, Meier A, Edwards GR (1996) Mater Sci Eng 206:250
17. Jason TC, Mangesh T, Abhaya B, Datye K, Davis JR (2006) J Catal 238:462
18. Szailer T, Kwak JH, Kim DH, Hanson CJ, Peden CHF, Szanyi J (2006) J Catal 239:55. doi:10.1016/j.jcat.2006.01.014
19. Verrier LC, Bazin P, Saussey J, Daturi M (2003) Phys Chem 5:4425
20. Miyadera T (1998) Appl Catal B Environ 16:158
21. Sylvie LK, Legros C, Claude C, Herbst F (2006) J Eur Soc 26:2225
22. Loddo V, Marcì G, Palmisano L, Sclafani A (1998) Mater Chem Phys 53:220. doi:10.1016/S0254-0584(98)00041-8
23. Macleod N, Cropley R, Keel J, Lambert M (2004) J Catal 221:29. doi:10.1016/j.jcat.2003.07.005
24. Huang HY, Long RQ, Yang RT (2001) Appl Catal B Environ 33:127
25. Jiang XY, Lu GL, Zhou RX, Mao JX, Chen Y, Zheng XM (2001) Appl Surf Sci 173:212
26. Christodoulakis A, Machli M, Angeliki B, Lemonidou A, Boghosian S (2004) J Catal 222:293. doi:10.1016/j.jcat.2003.10.007
27. Lietti INL, Tronconi LCE, Forzatti P (2006) J Catal 239:247
28. Pike J, Chan SW, Zhang F, Wang XQ, Hanson J (2006) Appl Catal Gen 303:275. doi:10.1016/j.apcata.2006.02.008
29. Wu Y, Zhao Z, Liu Y, Yang XG (2000) J Mol Catal Chem 155:94. doi:10.1016/S1381-1169(99)00322-2
30. Li HJ, Jiang XY, Zheng XM (2006) Acta Phys-Chim Sin 22:587
31. Hu YH, Liu TD, Shen MM (2003) J Solid State Chem 170:66. doi:10.1016/S0022-4596(02)00020-8
32. Xu B, Dong L, Chen Y (1998) J Chem Soc Faraday Trans 94:907
33. Boccuzzi F, Chiorino A, Martra G, Gargano M, Ravasio N, Carrozziniz B (1997) J Catal 165:129. doi:10.1006/jcat.1997.1475
34. Wei ZB, Xin Q, Guo XX (1990) Appl Catal Gen 63:310
35. Vargas A, Montoya J, Maldonado C, Hernández-pérez I, Acosta D, Morales R (2004) Micro Mater 74:9
36. Luo MF, Fang P, He M, Xie YL (2005) J Mol Catal Chem 239:248. doi:10.1016/j.molcata.2005.06.029
37. Jiang XY, Ding GH, Lou LP, Chen YX, Zheng XM (2004) J Mol Catal Chem 218:193
38. Larssin PO, Andersson A (1998) J Catal 179:301
39. Li C, Li MJ (2002) J Raman Spectrosc 33:301
40. Davydov AA, Budneva AA, Sokolovski VD (1990) Kinet Catal 30:1224
41. Sica A, Gigola C (2003) Appl Catal Gen 239:121. doi:10.1016/S0926-860X(02)00380-0
42. Macleod N, Cropley R, Keel J, Lambert M, Richard M (2004) J Catal 221:20. doi:10.1016/j.jcat.2003.07.005
43. Dictor RWJ (1989) J Catal 109:89. doi:10.1016/0021-9517(88)90187-X
44. Novak E, Solymosi F (1990) J Catal 125:112. doi:10.1016/0021-9517(90)90082-U
45. London JW, Bell ATJ (1973) Catal 31:100
46. Sica AM, Gigola CE (2003) Appl Catal Gen 239:125. doi:10.1016/S0926-860X(02)00380-0